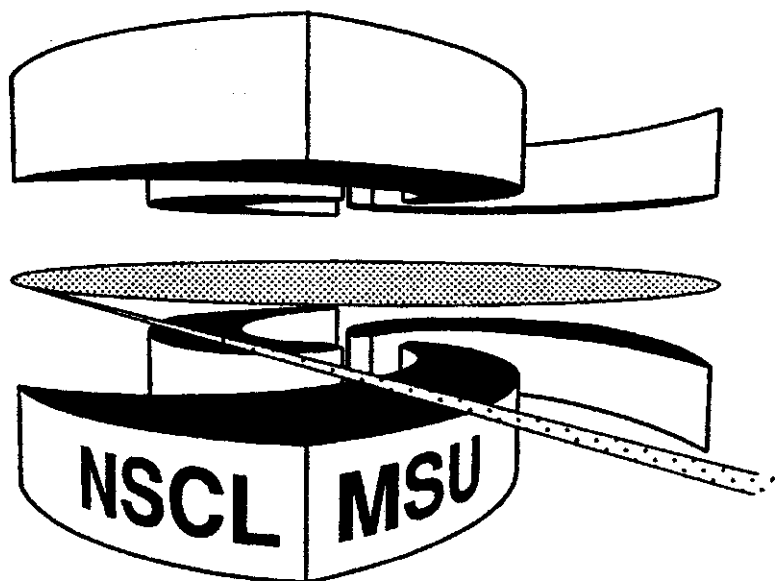


**MICHIGAN STATE**  
**UNIVERSITY**

**National Superconducting Cyclotron Laboratory**

**CORE EXCITATION IN COULOMB BREAKUP REACTIONS**

**R. SHYAM and P.DANIELEWICZ**



**MSUCL-1188**

**JANUARY 2001**

# Core excitation in Coulomb breakup reactions

R. Shyam<sup>a,b</sup> and P. Danielewicz<sup>a</sup>

<sup>a</sup> *National Superconducting Cyclotron Laboratory and  
Department of Physics and Astronomy, Michigan State University,  
East Lansing, Michigan 48824, USA*

<sup>b</sup> *Saha Institute of Nuclear Physics, Calcutta 700064, India*

(January 16, 2001)

Within the pure Coulomb breakup mechanism, we investigate the one-neutron removal reaction of the type  $A(a,b\gamma)X$  with  $^{11}\text{Be}$  and  $^{19}\text{C}$  projectiles on a heavy target nucleus  $^{208}\text{Pb}$  at the beam energy of 60 MeV/nucleon. Our intention is to examine the prospective of using these reactions to study the structure of neutron rich nuclei. Integrated partial cross sections and momentum distributions for the ground as well as excited bound states of core nuclei are calculated within the finite range distorted wave Born approximation as well as within the adiabatic model of the Coulomb breakup. Our results are compared with those obtained in the studies of the reactions on a light target where the breakup proceeds via the pure nuclear mechanism. We find that the transitions to excited states of the core are quite weak in the Coulomb dominated process as compared to the pure nuclear breakup.

PACS numbers: 24.10.Eq., 25.60.-t, 25.60.Gc, 24.50.+g

KEYWORD: One-neutron removal reactions, structure of core excited states, finite range DWBA theory of Coulomb breakup.

## I. INTRODUCTION

The single-nucleon transfer reactions, induced by light as well as heavy ions, have been established as a useful tool in probing the single-particle components of the wave functions of stable nuclei (see e.g. [1–4]). The theory of these reactions developed within the framework of the distorted wave Born approximation (DWBA) [5] has been widely used to analyze the absolute magnitudes and shapes of measured cross sections and to deduce the structure information including angular momentum assignments, occupation probabilities and spectroscopic factors of the ground as well as excited states of the residual nuclei.

Nonetheless, transfer reactions are not yet routinely used in probing the structure of exotic nuclei near the neutron and proton drip lines, even though the first theoretical feasibility study [6] for such investigations with transfer reactions and the first experimental results [7] for the  $^{11}\text{Be}(p,d)^{10}\text{Be}$  reaction have been already reported. With the currently available experimental techniques, the measurements of these reactions involving drip line nuclei are performed in the inverse kinematics with low intensity projectile beams. This puts severe experimental restrictions as the corresponding cross sections are usually low. Furthermore, the theoretical analysis of these data in terms of the DWBA gets complicated as the usual well-depth search method to calculate the wave function of the transferred particle becomes unreliable [7], and the methods such as Skyrme Hartree-Fock theory need to be invoked [6] for a proper description of these wave functions.

Recently, an alternative new and more versatile technique for investigating the spectroscopy of nuclei near the drip line has been developed [8–11]. In this method, referred to as the  $(a,b\gamma)$  reaction in the following, one nucleon (usually the valence or halo) is removed from the projectile (a) in its breakup reaction within the field of a target nucleus. The states of the core fragment (b) populated in this reaction are identified by their gamma ( $\gamma$ ) decay. The  $\gamma$ -ray intensities are used to determine the partial breakup cross sections to different core states. The signatures of the orbital angular momentum  $\ell$  associated with the relative motion of core states with respect to the valence nucleon (removed from the projectile) are

provided by the measured parallel momentum distributions [12].

This method improves the experimental conditions for working with projectiles of low beam intensities because of: (i) large partial cross sections for transitions to various bound states of the core fragment, even in experiments done with high-energy projectiles, (ii) possibility of using thick targets, and (iii) strong forward focusing. These features may be contrasted with those of the corresponding transfer reactions. In addition, while, in the case of transfer reactions, the angular distributions of the ejectile lose their characteristic  $\ell$ -dependence at high energies [13], the longitudinal momentum distributions of the core states in the breakup reactions continue to show a strong dependence on  $\ell$ .

Most of the studies of the  $(a,b\gamma)$  reaction performed so far involve a light  ${}^9\text{Be}$  target, where the breakup process is governed almost entirely by only the nuclear interaction between the projectile fragments and the target. Since, this reaction is essentially inclusive in nature (as the measurements are performed only for the heavy core fragment), the nuclear partial cross sections have contributions from both elastic (also known as diffraction dissociation) and inelastic (also known as stripping or breakup-fusion) breakup modes [14,15]. Several attempts have been made to calculate the elastic and inelastic nuclear breakup cross sections of halo nuclei and they were either based on the semiclassical methods [16] or on the eikonal approximation [17–20]. The fragment-target interactions are dealt with differently in these two approaches which could be important for the light targets [21]. Data of Refs. [8–11] have been analyzed in terms of an eikonal model [22] with core-target and neutron-target interactions treated in the black disc approximation and in the optical limit of the Glauber theory, respectively. In order to extract unambiguous spectroscopic informations from the  $(a,b\gamma)$  type of measurements performed on a light target, it is quite desirable to develop the calculations of nuclear breakup reactions within the DWBA theory as has been done for the breakup of stable projectiles [23,24].

However, currently a full quantum mechanical theory of the pure Coulomb breakup reaction, formulated within the framework of the post-form distorted-wave Born-approximation, is well established and has been applied successfully to investigate the breakup of halo nuclei

[25]. Finite range effects are accounted for in this theory which can be applied to projectiles of any ground-state orbital angular-momentum structure. Moreover, an alternative theory of the Coulomb breakup reactions within the framework of an adiabatic model has also been formulated [26]. The expressions for the breakup amplitude within this theory are very similar to those of the finite-range DWBA theory, although the two have been derived under quite different assumptions. In the adiabatic model, it is assumed that the excited states of the projectile are degenerate with the ground state. In the studies of the breakup reactions done so far (where the core fragments were assumed to remain in their ground states), the two theories produced almost identical results [25]. However, with the excitation of the core, the one-neutron separation energies increase significantly. It would, therefore, be interesting to see if the two models lead to different results in these cases.

There are no adjustable parameter in either of the theories of pure Coulomb breakup reaction. Absence of the inelastic breakup mode in this case is an added advantage as there is some ambiguity regarding the calculation of this mode which dominates the partial cross sections for the excited core states in the nuclear breakup process [22].

In this paper, we present calculations of the pure Coulomb breakup contributions to the partial cross sections and longitudinal momentum distributions of the ground as well as excited states of the core fragments,  $^{10}\text{Be}$  and  $^{18}\text{C}$ , in the  $(a,b\gamma)$  type of reaction induced by  $^{11}\text{Be}$  and  $^{19}\text{C}$  projectiles, respectively on a  $^{208}\text{Pb}$  target at the beam energy of 60 MeV/nucleon. We assume that the states of the core fragments are the same as those seen in the similar reactions studied on the  $^9\text{Be}$  target. Our aim is to determine if there are quantitative differences in the *relative* populations of the core states in the pure Coulomb breakup mechanism, as compared to those observed in the pure nuclear breakup process. We shall also look whether there are differences in the predictions of the finite range DWBA and adiabatic models of the breakup reactions leading to the core excited states.

We want to make it clear from the very beginning that it is not our intention to imply that the nuclear breakup contributions are negligible for the reactions investigated by us. Our results should be viewed as complementing contributions from the nuclear breakup

process; in any complete theory both contributions must be considered on an equal footing.

In the next section we briefly present the formalism of the Coulomb breakup reactions. The results of our calculations and discussions are presented in section III. A summary and the conclusions of our work are given in section IV.

## II. FORMALISM

We consider the reaction  $a+t \rightarrow b+c+t$ , where the projectile  $a$  breaks up into fragments  $b$  (charged) and  $c$  (uncharged) in the Coulomb field of a target  $t$ . The chosen coordinate system is shown in Fig. 1.

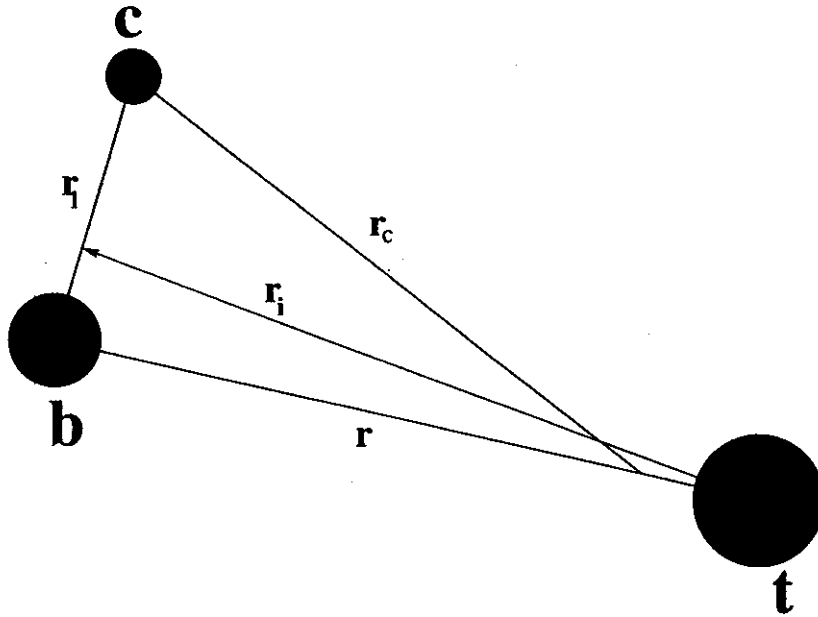


FIG. 1. The three-body coordinate system. The charged core, valence neutron and target are denoted by  $b$ ,  $c$  and  $t$ , respectively.

The position vectors satisfy the following relations:

$$\mathbf{r} = \mathbf{r}_i - \alpha \mathbf{r}_1, \quad \alpha = \frac{m_c}{m_c + m_b}, \quad (1)$$

$$\mathbf{r}_c = \gamma \mathbf{r}_1 + \delta \mathbf{r}_i, \quad \delta = \frac{m_t}{m_b + m_t}, \quad \gamma = (1 - \alpha\delta). \quad (2)$$

The starting point of both the finite-range distorted-wave Born approximation (FRD-WBA) and of the adiabatic model of the Coulomb breakup is the post-form  $T$ -matrix of the reaction given by

$$T = \int d\xi d\mathbf{r}_1 d\mathbf{r}_i \chi_b^{(-)*}(\mathbf{k}_b, \mathbf{r}) \Phi_b^*(\xi_b) \chi_c^{(-)*}(\mathbf{k}_c, \mathbf{r}_c) \Phi_c^*(\xi_c) V_{bc}(\mathbf{r}_1) \Psi_a^{(+)}(\xi_a, \mathbf{r}_1, \mathbf{r}_i). \quad (3)$$

The functions  $\chi$  are the distorted waves for the relative motions of  $b$  and  $c$  with respect to  $t$  and the center of mass (c.m.) of the  $b + t$  system, respectively. The functions  $\Phi$  are the internal state wave functions of the concerned particles dependent on the internal coordinates  $\xi$ . The function  $\Psi_a^{(+)}(\xi_a, \mathbf{r}_1, \mathbf{r}_i)$  is the exact three-body scattering wave function of the projectile with a wave vector  $\mathbf{k}_a$  satisfying outgoing boundary conditions. The vectors  $\mathbf{k}_b$  and  $\mathbf{k}_c$  are the Jacobi wave vectors of  $b$  and  $c$ , respectively, in the final channel of the reaction. The function  $V_{bc}(\mathbf{r}_1)$  represents the interaction between  $b$  and  $c$ . As we concentrate only on the pure Coulomb breakup, the function  $\chi_b^{(-)}(\mathbf{k}_b, \mathbf{r})$  is taken as the Coulomb distorted wave (for a point Coulomb interaction between the charged core  $b$  and the target) satisfying incoming wave boundary conditions, and the function  $\chi_c^{(-)}(\mathbf{k}_c, \mathbf{r}_c)$  is just a plane wave as there is no Coulomb interaction between the target and the neutral fragment  $c$ .

In the distorted wave Born approximation (DWBA), we write

$$\Psi_a^{(+)}(\xi_a, \mathbf{r}_1, \mathbf{r}_i) = \Phi_a(\xi_a, \mathbf{r}_1) \chi_a^{(+)}(\mathbf{k}_a, \mathbf{r}_i), \quad (4)$$

where the dependence of  $\Phi_a$  on  $\mathbf{r}_1$  describes the relative motion of the fragments  $b$  and  $c$  in the ground state of the projectile. The function  $\chi_a^{(+)}(\mathbf{k}_a, \mathbf{r}_i)$  is the Coulomb distorted scattering wave describing the relative motion of the c.m. of the projectile with respect to the target, satisfying outgoing wave boundary conditions. The assumption inherent in Eq. (4) is that the breakup channels are very weakly coupled and hence this coupling needs to be treated only in the first order.

The integration over the internal coordinates  $\xi$  in the  $T$ -matrix gives

$$\int d\xi \Phi_b^*(\xi_b) \Phi_c^*(\xi_c) \Phi_a(\xi_a, \mathbf{r}_1) = \sum_{\ell m j \mu} \langle \ell m j_c \mu_c | j \mu \rangle \langle j_b \mu_b j \mu | j_a \mu_a \rangle i^\ell \Phi_a(\mathbf{r}_1), \quad (5)$$

with

$$\Phi_a(\mathbf{r}_1) = u_\ell(r_1) Y_{\ell m}(\hat{\mathbf{r}}_1). \quad (6)$$

In Eq. (6),  $\ell$  (the orbital angular momentum for the relative motion between fragments  $b$  and  $c$ ) is coupled to the spin of  $c$  and the resultant channel spin  $j$  is coupled to the spin  $j_b$  of the core  $b$  to yield the spin of  $a$  ( $j_a$ ). The  $T$ -matrix can now be written as

$$T = \sum_{\ell m j \mu} \langle \ell m j_c \mu_c | j \mu \rangle \langle j_b \mu_b j \mu | j_a \mu_a \rangle i^{\ell} \hat{\ell} \beta_{\ell m}(\mathbf{k}_b, \mathbf{k}_c; \mathbf{k}_a), \quad (7)$$

where

$$\hat{\ell} \beta_{\ell m}(\mathbf{k}_b, \mathbf{k}_c; \mathbf{k}_a) = \int d\mathbf{r}_1 d\mathbf{r}_i \chi_b^{(-)*}(\mathbf{k}_b, \mathbf{r}) e^{-i\mathbf{k}_c \cdot \mathbf{r}_c} V_{bc}(\mathbf{r}_1) u_{\ell}(r_1) Y_{\ell m}(\hat{r}_1) \chi_a^{(+)}(\mathbf{k}_a, \mathbf{r}_i). \quad (8)$$

with  $\beta_{\ell m}$  being the reduced  $T$ -matrix and with  $\hat{\ell} \equiv \sqrt{2\ell + 1}$ .

Equation (8) involves a six dimensional integral which makes the computation of  $\beta_{\ell m}$  quite complicated. The problem gets further acute because the integrand has a product of three scattering waves that exhibit an oscillatory behavior asymptotically. Therefore, approximate methods have been used, such as the zero range approximation (see e.g. [1,2,4]), in which the product  $V_{bc}(\mathbf{r}_1)\Phi_a(\mathbf{r}_1)$  is replaced by a delta function, or the Baur-Trautmann approximation [27], where the projectile c.m. coordinate is replaced by that of the core-target system (i.e.  $\mathbf{r}_i \approx \mathbf{r}$ ). Both these approximations lead to a factorization of the reduced amplitude into two independent parts, which reduces the computational complexity. However, both these methods have limitations and their application to the reactions of halo nuclei is questionable [25].

In the FRDWBA theory, the Coulomb distorted wave of particle  $b$  in the final channel is written as [25]

$$\chi_b^{(-)}(\mathbf{k}_b, \mathbf{r}) = e^{-i\alpha \mathbf{K} \cdot \mathbf{r}_1} \chi_b^{(-)}(\mathbf{k}_b, \mathbf{r}_i). \quad (9)$$

Equation (9) represents an exact Taylor series expansion about  $\mathbf{r}_i$  if  $\mathbf{K} = -i\nabla_{\mathbf{r}_i}$  is treated exactly. However, instead of doing this we employ a local momentum approximation [28,29], where the magnitude of momentum  $\mathbf{K}$  is taken to be

$$K(R) = \sqrt{\frac{2m}{\hbar^2}(E - V(R))}. \quad (10)$$



Here  $m$  is the reduced mass of the  $b-t$  system,  $E$  is the energy of particle  $b$  relative to the target in the c.m. system and  $V(R)$  is the Coulomb potential between  $b$  and the target separated by  $R$ . Thus, the magnitude of the momentum of  $\mathbf{K}$  is evaluated at some separation  $R$  which is held fixed for all the values of  $r$ . The value of  $R$  was taken to be equal to 10 fm. For reactions under investigation in this paper, the magnitude of  $K$  remains constant for distances larger than 10 fm [25]. Due to the peripheral nature of the breakup reaction, the region  $R \gtrsim 10$  fm contributes maximum to the cross section. In fact, the calculated cross sections change by only about 5% if  $R$  is varied between 5 to 10 fm and with a further increase in  $R$  the change is less than 1%. Furthermore, the results of the calculations for these reactions, at the beam energies under investigation, are almost independent of the choice of the direction of momentum  $\mathbf{K}$  [25]. Therefore, we have taken the directions of  $\mathbf{K}$  and  $\mathbf{k}_b$  to be the same in all the calculations presented in this paper. It may be remarked here that in Ref. [30] an approximation similar to Eq. (9) was applied to the Coulomb distorted wave of the incident channel. That procedure brings in two difficulties. Firstly, the choice of the direction of the local momentum is somewhat complicated as directions of the both fragments in the final channel will have to be brought into consideration. Secondly, the procedure may produce a deviation from the exact DWBA approximation.

On substituting Eq. (9) into Eq. (8), we obtain the following factorized form of the reduced amplitude

$$\hat{\ell}\beta_{\ell m}^{FRDWBA} = \left[ \int d\mathbf{r}_1 e^{-i(\gamma\mathbf{k}_c - \alpha\mathbf{K})\cdot\mathbf{r}_1} V_{bc}(\mathbf{r}_1) u_{\ell}(\mathbf{r}_1) Y_{\ell m}(\hat{\mathbf{r}}_1) \right] \times \left[ \int d\mathbf{r}_i \chi_b^{(-)*}(\mathbf{k}_b, \mathbf{r}_i) e^{-i\delta\mathbf{k}_c\cdot\mathbf{r}_i} \chi_a^{(+)}(\mathbf{k}_a, \mathbf{r}_i) \right]. \quad (11)$$

This amplitude differs from those in earlier studies [23] since it includes the interaction  $V_{bc}$  to all orders.

Recently, an alternative theory of the Coulomb breakup has been developed within the adiabatic (AD) model [26,31]. This theory assumes (i) that one of the fragments (the valence nucleon) is neutral so that the projectile interacts with the target only through the Coulomb interaction  $V_{bt}$  of the core fragment and the target nucleus, and (ii) that the

relative excitation energy  $E_{bc}$  of the b-c system is much smaller than the total incident energy so that  $E_{bc}$  can be replaced by the constant separation energy of the fragments in the projectile ground state. Following (ii) the continuum spectrum of the  $b - c$  system is assumed to be degenerate with the ground state. Under the above assumptions, the wave function  $\Psi_a^{(+)}(\xi_a, \mathbf{r}_1, \mathbf{r}_i)$  is found [31] in the form

$$\Psi_a^{(+AD)}(\xi_a, \mathbf{r}_1, \mathbf{r}_i) = \Phi_a(\xi_a, \mathbf{r}_1) e^{i\alpha \mathbf{k}_a \cdot \mathbf{r}_1} \chi_a^{(+)}(\mathbf{k}_a, \mathbf{r}) \quad (12)$$

It is clear that substitution of Eq. (12) to Eq. (3) will lead to a factored form (similar to Eq. (11)) of the reduced breakup amplitude. However, one limitation of this procedure should be brought into attention. For larger values of  $r_1$ , the wave function  $\Psi_a^{(+AD)}$  vanishes due to the presence of the factor  $\Phi_a(\mathbf{r}_1)$ , whereas there may still be contributions to the breakup from this region. It has been argued [26] that, due the presence of the interaction  $V_{bc}(r_1)$ , the post form breakup amplitude may not be sensitive to the domain where  $\Psi_a^{(+AD)}$  is inaccurate. However, since the wave functions for the relative motion of the fragments for  $\ell > 0$  values have a large spatial extension, the application of this model to such cases may test the need for the non-adiabatic corrections to the theory.

The reduced amplitude in the adiabatic model is given by,

$$\hat{\beta}_{\ell m}^{AD} = \left[ \int d\mathbf{r}_1 e^{-i(\mathbf{k}_c - \alpha \mathbf{k}_a) \cdot \mathbf{r}_1} V_{bc}(\mathbf{r}_1) u_\ell(\mathbf{r}_1) Y_{\ell m}(\hat{r}_1) \right] \times \left[ \int d\mathbf{r}_i \chi_b^{(-)*}(\mathbf{k}_b, \mathbf{r}_i) e^{-i\delta \mathbf{k}_c \cdot \mathbf{r}_i} \chi_a^{(+)}(\mathbf{k}_a, \mathbf{r}_i) \right] \quad (13)$$

It is obvious that this amplitude differs from that of the FRDWBA, Eq. (11), only in the form factor part (the first of the factors), which is evaluated here at the momentum transfer of  $(\mathbf{k}_c - \alpha \mathbf{k}_a)$ . Equation (13) can also be obtained in the DWBA model by making a local momentum approximation to the Coulomb distorted wave in the initial channel of a reaction and by evaluating the local momentum at  $R = \infty$  with the momentum direction being the same as that of the projectile. In both of the theories, the Coulomb interaction between the fragments  $b$  and the target is treated non-perturbatively. The adiabatic model does not make the weak coupling approximation of the DWBA. However, it necessarily requires one of the

fragments (in this case  $c$ ) to be neutral. In contrast, the FRDWBA model can, in principle, be applied to the cases where both of the fragments  $b$  and  $c$  are charged [28]. Furthermore, calculation of the nuclear breakup in the adiabatic model is not as comparatively trivial [31–33], as it is in the case of FRDWBA.

The triple differential cross section of the reaction is given by

$$\frac{d^3\sigma}{dE_b d\Omega_b d\Omega_c} = \frac{2\pi}{\hbar v_a} \rho(E_b, \Omega_b, \Omega_c) \sum_{\ell m} |\beta_{\ell m}|^2, \quad (14)$$

where  $\rho(E_b, \Omega_b, \Omega_c)$  is the appropriate [25,34] three-body phase space factor.

On substituting the Coulomb distorted waves,

$$\chi_b^{(-)*}(\mathbf{k}_b, \mathbf{r}_i) = e^{-\pi\eta_b/2} \Gamma(1 + i\eta_b) e^{-i\mathbf{k}_b \cdot \mathbf{r}_i} {}_1F_1(-i\eta_b, 1, i(k_b r_i + \mathbf{k}_b \cdot \mathbf{r}_i)), \quad (15)$$

$$\chi_a^{(+)}(\mathbf{k}_a, \mathbf{r}_i) = e^{-\pi\eta_a/2} \Gamma(1 + i\eta_a) e^{i\mathbf{k}_a \cdot \mathbf{r}_i} {}_1F_1(-i\eta_a, 1, i(k_a r_i - \mathbf{k}_a \cdot \mathbf{r}_i)), \quad (16)$$

into Eqs. (11) and (13), one gets for the triple differential cross section:

$$\frac{d^3\sigma}{dE_b d\Omega_b d\Omega_c} = \frac{2\pi}{\hbar v_a} \rho(E_b, \Omega_b, \Omega_c) \frac{4\pi^2 \eta_a \eta_b}{(e^{2\pi\eta_b} - 1)(e^{2\pi\eta_a} - 1)} |I|^2 4\pi \sum_{\ell} |Z_{\ell}|^2. \quad (17)$$

In Eqs. (15–17),  $\eta$ 's are the Coulomb parameters for the respective particles. In Eq. (17),  $I$  is the Bremsstrahlung integral [35] which can be evaluated in the closed form:

$$I = -i \left[ B(0) \left( \frac{dD}{dx} \right)_{x=0} (-\eta_a \eta_b) {}_2F_1(1 - i\eta_a, 1 - i\eta_b; 2; D(0)) \right. \\ \left. + \left( \frac{dB}{dx} \right)_{x=0} {}_2F_1(-i\eta_a, -i\eta_b; 1; D(0)) \right], \quad (18)$$

where

$$B(x) = \frac{4\pi}{k^{2(i\eta_a + i\eta_b + 1)}} \left[ (k^2 - 2\mathbf{k} \cdot \mathbf{k}_a - 2xk_a)^{i\eta_a} (k^2 - 2\mathbf{k} \cdot \mathbf{k}_b - 2xk_b)^{i\eta_b} \right], \quad (19)$$

$$D(x) = \frac{2k^2(k_a k_b + \mathbf{k}_a \cdot \mathbf{k}_b) - 4(\mathbf{k} \cdot \mathbf{k}_a + xk_a)(\mathbf{k} \cdot \mathbf{k}_b + xk_b)}{(k^2 - 2\mathbf{k} \cdot \mathbf{k}_a - 2xk_a)(k^2 - 2\mathbf{k} \cdot \mathbf{k}_b - 2xk_b)}, \quad (20)$$

with

$$\mathbf{k} = \mathbf{k}_a - \mathbf{k}_b - \delta\mathbf{k}_c. \quad (21)$$

The factor  $Z_\ell$  contains the projectile structure information and is given by

$$Z_\ell = \int dr_1 r_1^2 j_\ell(k_1 r_1) V_{bc}(\mathbf{r}_1) u_\ell(r_1), \quad (22)$$

with  $k_1 = |\gamma\mathbf{k}_c - \alpha\mathbf{K}|$ , and  $k_1 = |\mathbf{k}_c - \alpha\mathbf{k}_a|$  for the cases of FRDWBA and adiabatic model, respectively.

The total pure Coulomb one-nucleon removal cross section for a given  $n\ell j$  configuration of the valence nucleon is obtained by integrating Eq. (13) over angles and energy of fragment  $b$  and over angles of the valence nucleon. Here,  $n$  is the principal quantum number and  $\ell$  and  $j$  are as defined in Eq. (5).

For calculating the total cross section into a given core-fragment final-state, the projectile ground state is described as having a configuration in which a valence nucleon, with single particle quantum numbers  $n\ell j$  and an associated spectroscopic factor  $C^2S$ , is coupled to a specific core state designated with  $j_b$  in Eq. (5). The total cross section  $\sigma_C$  is the sum [8,22] of the cross sections calculated with configurations (having non-vanishing spectroscopic factors) corresponding to all the allowed values of the channel spin  $j$

### III. RESULTS AND DISCUSSIONS

#### A. Excitation of the bound states of $^{10}\text{Be}$ in the Coulomb breakup of $^{11}\text{Be}$ .

The one-neutron removal reaction of the type  $^9\text{Be}(^{11}\text{Be}, ^{10}\text{Be}\gamma)X$  has been recently studied [9] at the beam energy of 60 MeV/nucleon. Partial cross sections have been measured for four states of the core fragment  $^{10}\text{Be}$ :  $0^+$ ,  $2^+$ ,  $1^-$ , and  $2^-$ . The data were analyzed in terms of an eikonal model of the nuclear breakup reactions [19,22], with the spectroscopic factors taken from [36]. It has been concluded in this study that about 22% of the total partial cross section went into the excited states, and that the ground state of  $^{11}\text{Be}$  consists of an admixture of the  $1s$  and  $0d$  single particle neutron configurations with the spectroscopic factors of 0.74 and 0.18, respectively.

We have calculated the pure Coulomb partial cross sections  $\sigma_C$  to the four  $^{10}\text{Be}$  final states in the  $^{208}\text{Pb}(^{11}\text{Be}, ^{10}\text{Be}\gamma)X$  reaction at the beam energy of 60 MeV/nucleon. The ground ( $0^+$ ) and excited (3.368 MeV) ( $2^+$ ) states were assumed to correspond to the configurations  $[1s_{1/2}\nu \otimes 0^+(^{10}\text{Be})]$  and  $[0d_{5/2}\nu \otimes 2^+(^{10}\text{Be})]$ , respectively, where  $\nu$  represents a relative neutron state. The corresponding  $C^2S$  values for these two configurations were taken [36] to be 0.74 and 0.20, respectively, i.e. the same as those used in [9]. The excited  $1^-$  (5.956 MeV) and  $2^-$  (6.256 MeV) states were assumed to stem from the configurations  $[0p_{3/2}\nu \otimes 1^-(^{10}\text{Be})]$  and  $[0p_{3/2}\nu \otimes 2^-(^{10}\text{Be})]$ , respectively, with the corresponding  $C^2S$  values of 0.69 and 0.58. These states could, in principle, also result from the stripping of a  $1p_{3/2}$  neutron from the  $^{10}\text{Be}(0^+)$  core of the  $^{11}\text{Be}$  ground state, producing a  $[1s_{1/2} \otimes ^9\text{Be}(\frac{3}{2})^-]1^-$  and  $[1s_{1/2} \otimes ^9\text{Be}(\frac{3}{2})^-]2^-$  types of  $^{10}\text{Be}^*$  core. In the nuclear breakup case, the cross sections to  $1^-$  and  $2^-$  states calculated with the latter configurations were found [22] to be about 10-15% smaller than those obtained with the preceding ones. We have carried out our calculations with the former configuration for these states. The one-neutron separation energy for the ground state of  $^{11}\text{Be}$ , with the configuration in which  $^{10}\text{Be}$  remains in its ground state, is taken to be  $S_n = 0.504$  MeV. For an excited state, the respective separation energy (SE) is assumed to be the sum of  $S_n$  and the excitation energy of that state with respect to the ground state.

In each case, the neutron single particle wave function is calculated in a central Woods-Saxon well of radius 1.15 fm and diffuseness 0.50 fm. The depth of this well is adjusted to reproduce the corresponding value of SE. By this procedure the root mean square (rms) radius of the ground state of  $^{11}\text{Be}$  comes out to be 2.91 fm for the assumed rms radius of the  $^{10}\text{Be}$  core of 2.28 fm.

Our results for the partial cross sections are shown in Table I. It is evident from this table that in the case of pure Coulomb breakup of a projectile with a halo ground state, most of the cross section goes to the ground state ( $0^+$ ) of the core. The sum of the partial cross sections corresponding to all the excited states is less than 1% of that to the ground state. This is in sharp contrast to the observations made on lighter targets where partial

cross sections corresponding to all the excited states represent about 22% of the total. While there are no experimental data on the core-excitation reaction induced by  $^{11}\text{Be}$  on a heavy target in the vicinity of  $^{208}\text{Pb}$ , the measurements [37] of the  $(a,b\gamma)$  type of reactions with  $^{14}\text{B}$  projectile on  $^{197}\text{Au}$  gold target at the beam energy of 60 MeV/nucleon may be used to test our results. In this experiment, no core-excited transitions were seen. Therefore, this lends support to our finding that in the  $A(a,b\gamma)X$  type of reactions, involving projectiles which have a predominant  $s$ -wave neutron halo ground state and a non- $s$ -wave core excited state, the transitions to the excited states of the core are quite weak in the pure Coulomb breakup reaction as compared to those in the nuclear breakup process.

The suppression of the cross sections to the higher states can be traced back to the strong dependence of the Coulomb breakup cross sections on  $SE$ . The latter enters in the corresponding expressions through the momentum  $k$  (see Eq. (21)). As was shown in [38], the modulus square of the bremsstrahlung integral  $I$  rises very steeply as the  $k$  approaches zero, which happens as  $SE$  goes to zero ( $|I|^2$  is infinite for  $k = 0$ ).

TABLE I. Calculated partial cross sections to the final states of  $^{10}\text{Be}$  in the Coulomb breakup of  $^{11}\text{Be}$  on the  $^{208}\text{Pb}$  target at the beam energy of 60 MeV/nucleon.  $I^\pi$  represents the spin and parity of the populated states of the  $^{10}\text{Be}$  core.

$I^\pi$	$E_x$ (MeV)	$\ell$	$C^2S$	$\sigma_C^{FRDWBA}$ (mb)	$C^2S \cdot \sigma_C^{FRDWBA}$ (mb)
$0^+$	0.0	0	0.74	1536.48	1137.00
$2^+$	3.368	2	0.20	2.09	0.42
$1^-$	5.956	1	0.69	2.45	1.69
$2^-$	6.256	1	0.58	2.07	1.20
		sum		6.69	3.31

At larger values of SE (i.e. larger  $k$ ) the rate of the drop of  $|I|^2$  becomes less drastic. This is reminiscent of the behavior of the virtual photon numbers in the theory of Coulomb excitation (see e.g. [40]). The value of  $k$  is very small for SE equal to  $S_n$  and larger for SE corresponding to excited states. This explains the reduction in the partial cross-sections to the excited  $2^+$  state of  $^{10}\text{Be}$  core as compared to that to its ground state. This also explains why the cross sections to the excited states do not differ much from each other. It may be useful to recall that, due to the centrifugal barrier, the breakup cross sections for non- $s$ -wave projectiles are lower than those for the  $s$ -wave ones. In case of the nuclear breakup, the dependence of the cross section on SE is comparatively weaker [16,39,41]. This could be understood from the fact that nuclear breakup cross sections are sensitive to the  $b - c$  relative wave functions at shorter distances which do not change much with changes in the value of SE.

It should be interesting to compare the calculated pure Coulomb partial cross section for the  $^{197}\text{Au}(^{14}\text{B}, ^{13}\text{B}(\text{g.s}))\text{X}$  reaction, with its experimental value given in Ref. [37]. We performed our calculations with the configurations  $[1s_{1/2}\nu \otimes \frac{3}{2}^-(^{13}\text{B})]$  and  $[0d_{5/2}\nu \otimes \frac{3}{2}^-(^{13}\text{B})]$  for the  $^{14}\text{B}$  ground state. The resulting cross sections were summed up, after multiplying them with the corresponding spectroscopic factors of 0.663 and 0.306 (taken from [36]), respectively, to obtain a value of 401 mb for the pure Coulomb partial cross section for this reaction. The corresponding experimental value is  $638 \pm 45$  mb. The difference between the calculated pure Coulomb and experimental partial cross sections suggests that the nuclear, and Coulomb-nuclear interference terms could contribute up to 40-50% in this reaction. This is an interesting finding which underlines the need for extending the FRDWBA theory to include the nuclear breakup effects. It should be stated here, that the partial Coulomb cross sections obtained within the adiabatic model are only a few percent larger than those of the FRDWBA theory and show similar characteristics to those in Table I.

The longitudinal momentum distributions (LMD) for each of the  $^{10}\text{Be}$  core state are displayed in Fig. 2. The solid and dashed lines represent the results of the FRDWBA and adiabatic model, respectively. We note that, while for the ground state of the  $^{10}\text{Be}$  core,

the results of the two theories are almost identical, they differ quite a bit from each other for the excited states. It is for the first time that such big differences are seen between the predictions of the two theories for the momentum distributions.

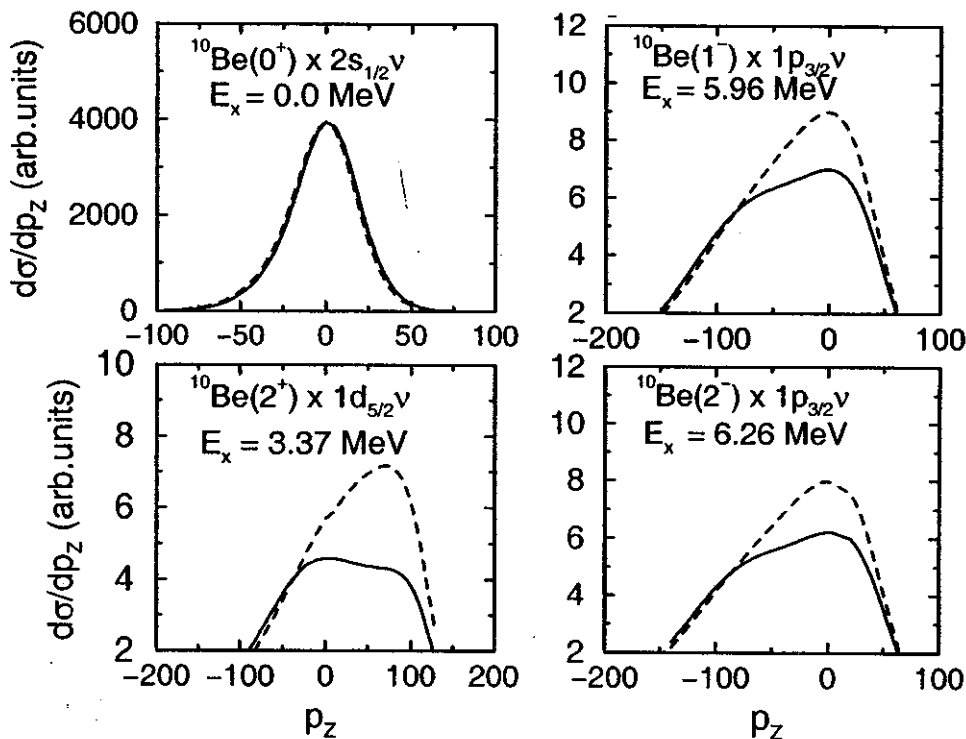


FIG. 2. Partial longitudinal momentum distributions for the indicated states of  $^{10}\text{Be}$  fragment in the pure Coulomb one neutron removal reaction of  $^{11}\text{Be}$  on a  $^{208}\text{Pb}$  target at the beam energy of 60 MeV/nucleon. The solid and dashed lines represent the results obtained within FRDWBA and adiabatic models respectively. The core - valence neutron configuration considered for each state is indicated in the respective boxes.

Although due to unavailability of the experimental data for these cases, it would be premature to comment upon suitability of either theory for these excited states, a few speculative remarks can still be made. It is not unreasonable to think that the adiabatic assumption (as discussed in the previous section) may come under severe pressure for the excited states. Due to their non- $s$ -wave nature, the wave functions for the excited-state neutron-core motion peak at larger values in the  $r$ -space yielding possibly a significance to the regime where the asymptotic form of the adiabatic wave function (11) becomes inadequate. It would,



therefore, be interesting to investigate the importance of the non-adiabatic corrections [33] to the theory, for these cases.

The full width at half maximum (FWHM) of the calculated LMD for the ground state of  $^{10}\text{Be}$  is 44 MeV/c which is consistent with the experimental value of  $(47.5 \pm 6)$  MeV/c seen in the measurements on a  $^9\text{Be}$  target [9]. This reconfirms that LMDs are independent of the reaction mechanism and provide a very clean way of determining the existence of halo structure in nuclei. The LMDs for the excited states of  $^{10}\text{Be}$  are broad which is also consistent with the observations made in [9]. This indicates that the respective states have a non-halo structure.

### B. Excitation of the bound states of $^{18}\text{C}$ in the Coulomb breakup of $^{19}\text{C}$ .

Table II displays results of our calculations of the pure Coulomb partial cross sections  $\sigma_C$  for transitions to ground and three excited bound states of  $^{18}\text{C}$  core in the  $^{208}\text{Pb}(^{19}\text{C}, ^{18}\text{C}\gamma)\text{X}$  reaction at the beam energy of 60 MeV/nucleon. These states have recently been seen [11] in the  $^9\text{Be}(^{19}\text{C}, ^{18}\text{C}\gamma)\text{X}$  reaction at the same beam energy.

TABLE II. Calculated partial cross sections to the final states of  $^{18}\text{C}$  in the Coulomb breakup of  $^{19}\text{C}$  on a  $^{208}\text{Pb}$  target at the beam energy of 60 MeV/nucleon.

$I^\pi$	$E_x$ (MeV)	$\ell$	$C^2S$	$\sigma_C$ (mb)	$C^2S \cdot \sigma_C$ (mb)
$0^+$	0.0	0	0.58	993.2	576.1
$2^+$	1.6	2	0.48	8.80	4.22
$0^+$	4.0	0	0.32	13.38	4.28
$2^+, 3^+$	4.9	2	2.44	1.08	2.87
		sum		23.26	11.37

The states of the  $^{18}\text{C}$  core (with excitation energies of 0.0 MeV, 1.6 MeV, 4.0 MeV and 4.9 MeV) are assumed to have the configurations,  $[1s_{1/2\nu} \otimes 0^+(^{18}\text{C})]$ ,  $[0d_{5/2\nu} \otimes 2^+(^{18}\text{C})]$ ,  $[1s_{1/2\nu} \otimes 0^+(^{18}\text{C})]$ , and  $[0d_{5/2\nu} \otimes 1^{\pi}(^{18}\text{C})]$ , respectively. The corresponding  $C^2S$  values were taken [36] to be 0.58, 0.48, 0.32 and 2.44, respectively, which are the same as those used in [11]. The value of  $S_n$  for the ground state was taken to be 0.530 MeV. We see that in this case too the ground state of  $^{18}\text{C}$  is predominantly excited. The partial cross sections to the excited states are somewhat larger than those seen in the case of  $^{10}\text{Be}$ , since the excited  $0^+$  state of  $^{18}\text{C}$  core can have an  $s$ -wave neutron relative motion. Yet, these contributions represent no more than about 2% of the cross section to the ground state.

The LMD for each of the  $^{18}\text{C}$  core states is shown in Fig. 3. The solid and dashed lines show the results of the FRDWBA and adiabatic models, respectively. In this case too we note that the predictions of the two models differ for the excited states of the core, while for the ground state they agree very well with each other.

The value of  $S_n$  for  $^{19}\text{C}$  is still an unsettled issue. The weighted average of the atomic mass measurements carried out at Los Alamos and GANIL [42,43] suggests a value of  $0.16 \pm 0.11$  MeV. However, from the analysis [44,45] of the data on the Coulomb dissociation of  $^{19}\text{C}$ , a higher value of 0.530 MeV has been extracted. The interpretation of the recent data [11] on the  $^9\text{Be}(^{19}\text{C}, ^{18}\text{C}\gamma)X$  reaction also suggests a higher value of  $0.8 \pm 0.3$  MeV. Obviously, any conclusion drawn from the breakup data strongly depends on the reaction mechanism and on the theory used for the calculation of the breakup cross sections. With this precaution, we would like to show here that the pure Coulomb breakup has some advantages over the nuclear breakup process in this regard.

It should be mentioned here that one of the reasons for the uncertainty in the value of  $S_n$  in Ref. [11] is the fact that, due to the low beam intensity in this experiment, the statistical errors associated with the measured LMD for the ground state of  $^{18}\text{C}$  are large. The data do not allow to distinguish between the nuclear breakup calculations of the LMD done within the range  $S_n = 800 \pm 300$  keV. The difference in the peak value of the nuclear LMD [11] calculated with  $S_n = 1100$  keV and 500 keV is only about 1.6. In contrast, the peak values

of the corresponding pure Coulomb LMD calculated with the same values of  $S_n$  differ by a factor of about 4, as can be seen in Fig. 4. This result is unlikely to be altered by the presence of the nuclear breakup effects, as they tend to show up in the tail regions of the LMDs. Thus  $A(^{19}\text{C}, ^{18}\text{C}(\text{g.s}))X$  type of reactions on a heavy target may offer a better chance to put more definite constraint on the value of  $S_n$  for  $^{19}\text{C}$ .

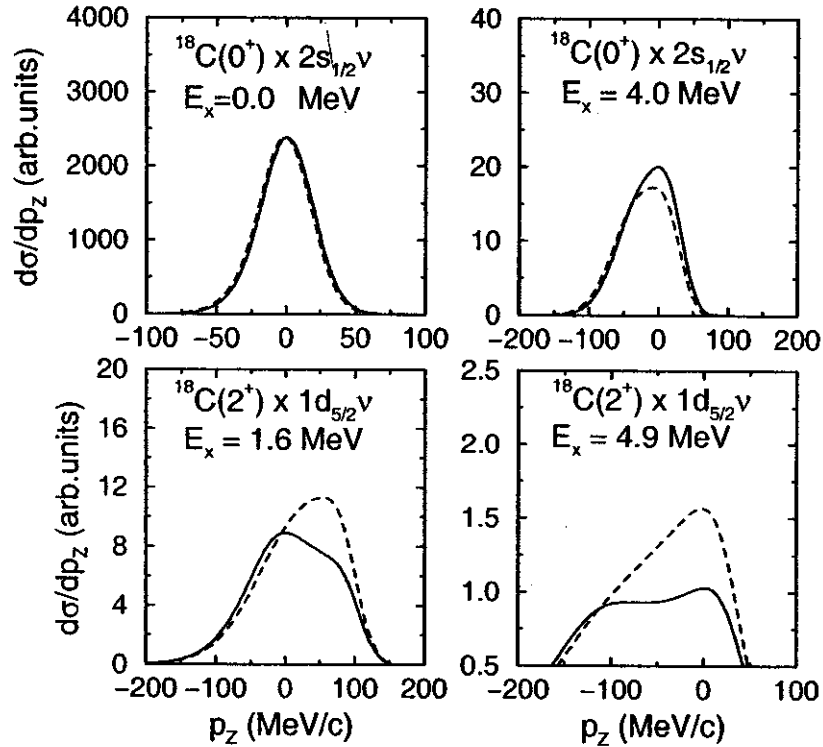


FIG. 3. Partial longitudinal momentum distributions for the indicated states of  $^{18}\text{C}$  fragment in the pure Coulomb one neutron removal reaction of  $^{19}\text{C}$  on a  $^{208}\text{Pb}$  target, at the beam energy of 60 MeV/nucleon. The solid and dashed lines represent the results obtained within the FRDWBA and adiabatic models, respectively. The core - valence neutron configuration considered for each state is indicated in the respective boxes.

Further insight into the value of  $S_n$  from these reactions can be obtained from the full width at half maximum (FWHM) of the LMD. In Fig. 5, we show the  $S_n$  dependence of the FWHM of the LMD for the  $^{18}\text{C}(\text{g.s})$  in the same reaction as in Fig. 4. It can be seen that FWHM increases from 42 MeV/c to about 65 MeV/c as  $S_n$  increases from 500 keV to 1100 keV. The variation of the corresponding FWHM in the nuclear breakup case is relatively

weaker.

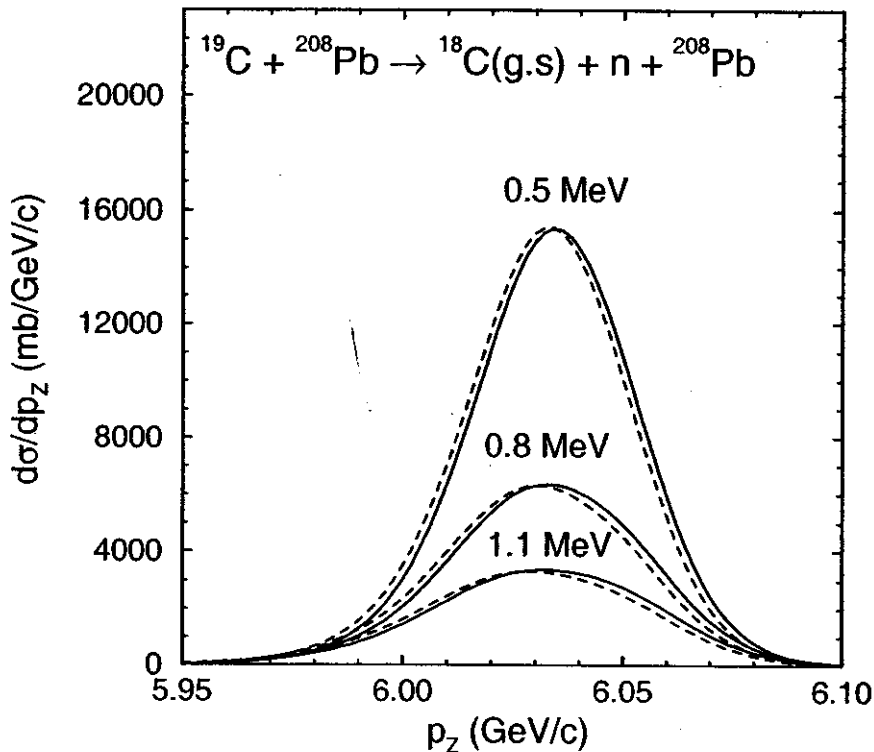


FIG. 4. Partial longitudinal momentum distribution for the ground state of  $^{18}\text{C}$  in the pure Coulomb one neutron removal reaction of  $^{19}\text{C}$  on a  $^{208}\text{Pb}$  target at the beam energy of 60 MeV/nucleon for the core - valence neutron separation energies of 0.5 MeV, 0.8 MeV and 1.1 MeV, as indicated. The solid and dashed curves represent the results of the FRDWBA and adiabatic models, respectively, in each case.

#### IV. SUMMARY AND CONCLUSIONS

In this paper we calculated the pure Coulomb breakup contributions to the partial cross sections and to the longitudinal momentum distributions for the ground and excited states of the core fragments observed in  $^{208}\text{Pb}(^{11}\text{Be},^{10}\text{Be}\gamma)\text{X}$  and  $^{208}\text{Pb}(^{19}\text{C},^{18}\text{C}\gamma)\text{X}$  types of one-neutron removal reactions, at the beam energy of 60 MeV/A. These reactions have recently been studied at the Michigan State University but on the light  $^9\text{Be}$  target; hence, these data are dominated by the nuclear breakup effects. One of our aims was to see in what

way the Coulomb dominated reaction mechanism was different and could supplement the conclusions derived from the pure nuclear breakup studies of the nuclei. The advantage of the pure Coulomb break up process is that the corresponding theory has no free adjustable parameter, and that the inelastic breakup mode does not contribute to this process.

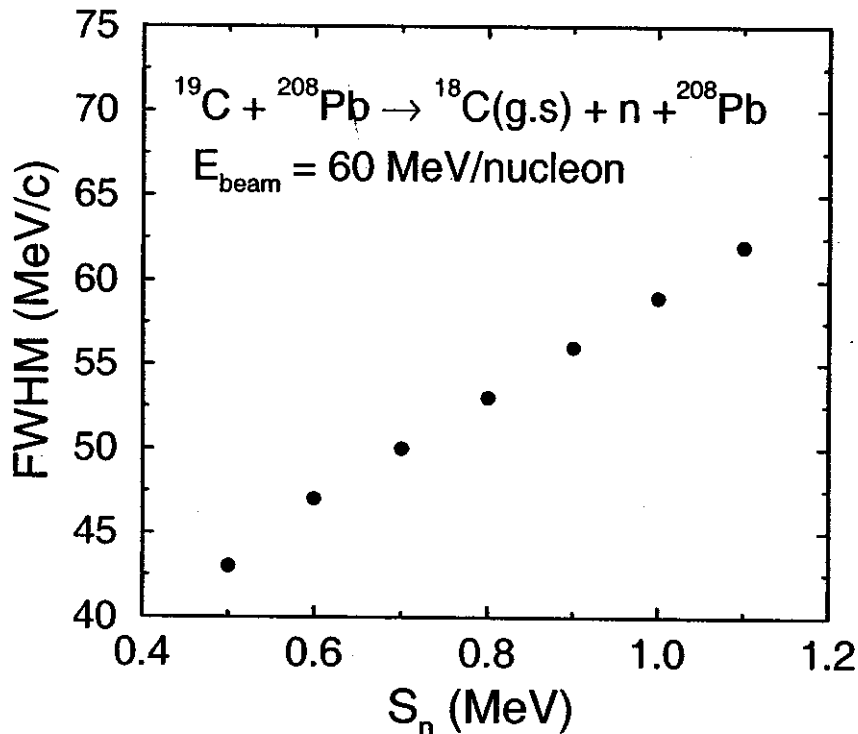


FIG. 5. Full width at half maximum (FWHM) of the longitudinal momentum distribution of  $^{18}\text{C}(\text{g.s})$  (shown by solid circles) as a function of the core - valence neutron separation energy in the same reaction as in Fig. 4. The FRDWBA and adiabatic model results are indistinguishable from each other.

As in the previous studies [10,9,11], we assumed that the coupling between the core states is weak and that there is no dynamical excitation of these states. Thus, the reaction can only populate those core states which have a non-zero spectroscopic factor for a given neutron-core configuration in the projectile ground state. We employed both the finite range DWBA and adiabatic model of the Coulomb breakup theory in our calculations. In earlier studies [25] of the inclusive Coulomb dissociation cross sections, the two theories produced

nearly identical results for the momentum distributions of heavy fragments.

We found that in reactions of the type  $A(a,b\gamma)X$  on a heavy target, the core ground state is predominantly excited; higher energy states account for only a few percent of the total cross section. This finding is in contrast to the results obtained on similar reactions on a light target, where about a quarter of the total breakup cross section could be due to transitions to core excited states. Our finding is supported by a recent measurement [37] of the  $^{197}\text{Au}(^{14}\text{B},^{13}\text{B}\gamma)X$  reaction at the beam energy of 60 MeV. The reason for this difference is attributed to the fact that pure Coulomb breakup cross sections drop very strongly as the separation energy increases. On the other hand, the nuclear breakup cross sections decrease slowly with increasing SE. Therefore, such reactions on a heavy target are potentially a more useful tool for investigating the properties of the ground state of the core fragments.

A rather interesting result of our study is that the finite-range DWBA and the adiabatic theories of Coulomb breakup lead to very different longitudinal momentum distributions for the excited states of the core fragments. It is probably for the first time that such a large difference is seen in the predictions of two theories for the momentum distributions. This should provide some impetus to look for the non-adiabatic corrections to the adiabatic approximation which may come under some pressure for the excited states.

Coulomb dominated breakup reactions may provide a better way for resolving the uncertainty associated with the one neutron separation energy of  $^{19}\text{C}$ . The peak value and the full width at half maximum of the longitudinal momentum distributions for the ground state of  $^{18}\text{C}$  core are more sensitive to the one-neutron separation energy in the Coulomb breakup process than in the nuclear breakup. In the latter case, the dependence could be so weak that the data with limited statistics may not allow to distinguish between the values of these quantities calculated with quite different one-neutron separation energies.

One of the authors (RS) would like to acknowledge several useful discussions with Gregers Hansen. This work was supported by the National Science Foundation under Grant PHY-0070818.

- 
- [1] G. R. Satchler, *Direct Nuclear Reactions*, (Oxford University Press, New York, 1983).
- [2] N. Austern, *Direct Nuclear Reactions Theory*, (Wiley, New York, 1970).
- [3] H. Feshbach, *Theoretical Nuclear Physics, Vol. 2*, (Wiley, New York, 1992).
- [4] N. Glendenning, *Direct Nuclear Reaction*, (Academic 1983).
- [5] G.R. Satchler, Nucl. Phys. 55, 1 (1964).
- [6] H. Lenske and G. Schrieder, Eur. Phys. J. A2, 41 (1998).
- [7] J.S. Winfield *et al.*, Nucl. Phys. A (in Press).
- [8] A.Navin *et al.*, Phys. Rev. Lett. 81, 5089 (1998).
- [9] T. Aumann *et al.*, Phys. Rev. Lett. 84, 35 (2000).
- [10] A. Navin *et al.*, Phys. Rev. Lett. 85, 266 (2000).
- [11] V. Maddalena *et al.*, Preprint, Michigan State University, MSUCL-1171 (2000), Phys. Rev. C (in press).
- [12] P.G. Hansen, Phys. Rev. Lett. 77, 1016 (1996).
- [13] A. Boudard *et al.*, Phys. Rev. Lett. 46, 218 (1981); R.P. Liljestrang *et al.*, Phys. Lett. 99B, 311 (1981); T.S. Baur *et al.*, Phys. Rev. C 21, 757 (1980).
- [14] G. Baur, S. Typel, H.H. Wolter, K. Henken and D. Trautmann, LANL preprint nucl-th/0001045.
- [15] A. Kasano and M. Ichimura, Phys. Lett. 115B, 81 (1982).
- [16] A. Bonaccorso and D.M. Brink, Phys. Rev. C 38, 1776 (1988); *ibid* Phys. Rev. C 58, 2864 (1998); A. Bonaccorso, Phys. Rev. C 60, 054604 (1999); A. Bonaccorso and F. Carstoiou,

Phys. Rev. C **61**, 034605 (2000).

- [17] K. Yabana, Y. Ogawa, and Y. Suzuki, Nucl. Phys. **A539**, 295 (1992);
- [18] K. Henken, G.F. Bertsch, and H. Esbensen, Phys. Rev. C **54**, 3043 (1996); G.F. Bertsch, K. Henken and H. Esbensen, Phys. Rev. C **57**, 1366 (1998); H. Esbensen and G. Bertsch, Phys. Rev. C **59**, 3240 (1999).
- [19] F. Barranco, E. Vigezzi, and R.A. Broglia, Z. Phys. A **356**, 45 (1996).
- [20] Yu. L. Parfenova, M.V. Zhukov, and J.S. Vaagen, Phys. Rev. C **62**, 044602 (2000).
- [21] A. Bonaccorso and G.F. Bertsch, LANL preprint nucl-th/0011062.
- [22] J. A. Tostevin, J. Phys. G: Nucl. Part. Phys. **25**, 735 (1999).
- [23] G. Baur, F. Rösler, D. Trautmann, and R. Shyam, Phys. Rep. **111**, 333 (1984).
- [24] M.H. Hussein and K.W. McVoy, Nucl. Phys. **A445**, 124(1985).
- [25] R. Chatterjee, P. Banerjee and R. Shyam, Nucl. Phys. **A675**, 477 (2000).
- [26] J. A. Tostevin, S. Rugmai, and R. C. Johnson, Phys. Rev. C **57**, 3225 (1998); J. A. Tostevin et al., Phys. Lett. **B424**, 219 (1998).
- [27] G. Baur and D. Trautmann, Nucl. Phys. A **A191**, 321 (1972).
- [28] R. Shyam and M.A. Nagarajan, Ann. Phys. (NY) **163**, 285 (1985).
- [29] P. Braun-Munzinger and H.L. Harney, Nucl. Phys. **A233** (1974) 381.
- [30] P. Banerjee, I.J. Thompson, and J. Tostevin, Phys. Rev. C **58**, 1042 (1998).
- [31] R.C. Johnson, J.S. Al-Khalili, and J.A. Tostevin, Phys. Rev. Lett. **79**, 2771 (1997).
- [32] J.A. Christley, J.S. Al-Khalili, J.A. Tostevin, and R.C. Johnson, Nucl. Phys. **A624**, 275 (1997)
- [33] R.C. Johnson, J. Phys. G **24**, 1583 (1998).



- [34] H. Fuchs, Nucl. Instrum. Methods **200**, 361 (1982).
- [35] A. Nordsieck, Phys. Rev. **93**, 785 (1954).
- [36] E.K. Warburton and B.A. Brown, Phys. Rev. C **46**, 923 (1992).
- [37] V. Guimarães et al., Phys. Rev. C **61**, 064609 (2000).
- [38] P. Banerjee and R. Shyam, Nucl. Phys. **A561**, 112 (1993).
- [39] R. Shyam, G. Baur and P. Banerjee, Phys. Rev. C **44**, 915 (1991).
- [40] C. Bertulani and G. Baur, Phys. Rep. **163**, 299 (1988).
- [41] C.H. Dasso, S.M. Lenzi, and A. Vitturi, Phys. Rev. C **59**, 539 (1999).
- [42] J. Wouters *et al.*, Z. Phys. A **331**, 229 (1988).
- [43] N. Orr *et al.*, Phys. Lett. **B258**, 29 (1991).
- [44] T. Nakamura *et al.*, Phys. Rev. Lett. **83**, 1112 (1999).
- [45] P. Banerjee and R. Shyam, Phys. Rev. C **61**, 047301 (2000).
- [46] G. Audi and A.H. Wapstra, Nucl. Phys. **A565**, 1 (1993); G. Audi, O. Bersillon, J. Blachot, and A.H. Wapstra, Nucl. Phys. **A624**, 1 (1997).

## Figure Captions

- Fig. 1 The three-body coordinate system. The charged core, valence neutron and target are denoted by  $b$ ,  $c$  and  $t$ , respectively.
- Fig. 2 Partial longitudinal momentum distributions for the indicated states of  $^{10}\text{Be}$  fragment in the pure Coulomb one neutron removal reaction of  $^{11}\text{Be}$  on a  $^{208}\text{Pb}$  target at the beam energy of 60 MeV/nucleon. The solid and dashed lines represent the results obtained within FRDWBA and adiabatic models respectively. The core - valence neutron configuration considered for each state is indicated in the respective boxes.
- Fig. 3 Partial longitudinal momentum distributions for the indicated states of  $^{18}\text{C}$  fragment in the pure Coulomb one neutron removal reaction of  $^{19}\text{C}$  on a  $^{208}\text{Pb}$  target, at the beam energy of 60 MeV/nucleon. The solid and dashed lines represent the results obtained within the FRDWBA and adiabatic models, respectively. The core - valence neutron configuration considered for each state is indicated in the respective boxes.
- Fig. 4 Partial longitudinal momentum distribution for the ground state of  $^{18}\text{C}$  in the pure Coulomb one neutron removal reaction of  $^{19}\text{C}$  on a  $^{208}\text{Pb}$  target at the beam energy of 60 MeV/nucleon for the core - valence neutron separation energies of 0.5 MeV, 0.8 MeV and 1.1 MeV, as indicated. The solid and dashed curves represent the results of the FRDWBA and adiabatic models, respectively, in each case.
- Fig. 5 Full width at half maximum (FWHM) of the longitudinal momentum distribution of  $^{18}\text{C}(\text{g.s.})$  (shown by solid circles) as a function of the core - valence neutron separation energy in the same reaction as in Fig. 4. The FRDWBA and adiabatic model results are indistinguishable from each other.